Optical Properties of Double-Shell Hollow ZnS-Ag2S Nanoparticles

ARTICLE *in* THE JOURNAL OF PHYSICAL CHEMISTRY C · NOVEMBER 2013

Impact Factor: 4.77 · DOI: 10.1021/jp408105m

2 AUTHORS:

Rajib Ghosh Chaudhuri
King Abdullah University of Science and Techn…
17 PUBLICATIONS **803** CITATIONS
SEE PROFILE

Santanu Paria
National Institute of Technology Rourkela
52 PUBLICATIONS **1,783** CITATIONS
SEE PROFILE

THE JOURNAL OF PHYSICAL CHEMISTRY C

Article

pubs.acs.org/JPCC

Optical Properties of Double-Shell Hollow ZnS−Ag_2S Nanoparticles

Rajib Ghosh Chaudhuri and Santanu Paria*

Interfaces and Nanomaterials Laboratory, Department of Chemical Engineering, National Institute of Technology, Rourkela 769008, Orissa, India

Supporting Information

ABSTRACT: The light emission properties of semiconductor nanoparticles are important for their applications in optical imaging, sensors, or lasers. ZnS nanoparticles are particularly useful for these applications, but the main hindrance for their widespread use are the low emission properties of pure ZnS nanoparticles. Formation of a core/shell structure is one way that has been used to improve the emission properties of pure ZnS in recent years. This study reports a unique synthesis route and the optical properties of double-shell ZnS−Ag_2S hollow nanoparticles. Light emission properties of hollow Ag_2S/ZnS are maximum (39%) compared to those of hollow ZnS/Ag_2S (21%) or pure ZnS (14%) nanoparticles, and these properties highly depend on the external ZnS layer thickness.

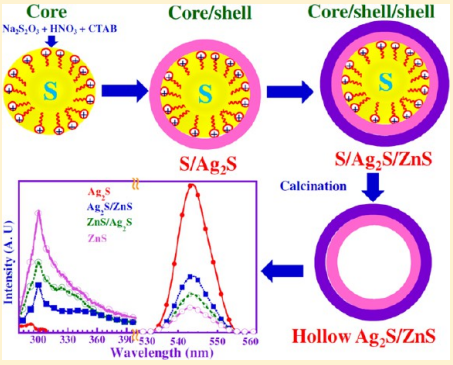

INTRODUCTION

The study of multishell nanoscale heterostructures in the form of a rattle[1] or a hollow[2−7] shape has been more focused in recent years because of their promising applications in plasmonic, catalytic, optical, and biomedical fields.[2,6,8] The properties of these particles can be tuned with respect to particle size, composition, sequence of shell layers, thickness of the individual shell layers, and so on. In most cases, these type of particles may also show dual properties, and so these particles are applicable in multiple ways, especially in multishell noble metals, semiconductor nanoparticles, magnetic, or metal oxide materials, which are extensively studied because of their wide range of applications in modern electronics, catalysis, and biomedical fields. The quantum yield (QY), response time, and the lifetime of the semiconductor materials at the applied environment are major important factors for any particular application.[9,10] The band gap and type of the semiconductor material (either direct or indirect) provide an idea regarding the stability and response time for designing these structures. Generally, direct semiconductor materials with a moderate band gap (~1.4−2.5 eV) are useful for the application in optical imaging or sensors because of the direct radiative transition between the excited and the valence state and the average stability.[11] In most of the recent applications of semiconductor nanomaterials, either single or multishell core/shell heterostructured materials are used instead of simple pure semiconductor materials.[10] The advantages of multishell nanoparticles over pure or single-shell core/shell nanoparticles are mainly improved optical properties (including higher quantum yield, higher photoluminescence efficiency) and an increased half-life of the semiconductor materials, which in turn increase the efficiency of these materials in different applications.[9,10] Additionally, other advantages include the easy detection in bioimaging because of the shifting of emission spectra toward higher wavelengths (visible range), better photo-oxidation stability, improved relevant electronic properties (band gap, band alignment), and better structural (lattice mismatch) properties than those of pure and even single-shell core/shell nanoparticles. Studies on multilayer hollow nanoparticles are rare, but multilayer core/shell nanoparticles, especially semiconductor-based[12−17] or combinations of semiconductor and other materials such as metal and metal oxides,[18−21] have been studied by different research groups.

In general, the photoluminescence properties of semiconductor materials are utilized extensively in biomolecular diagnostics, ultrasensitive in vitro assays for optical imaging,[22−24] and chemical detector[25−28] applications. Among several semiconductor nanoparticles, ZnS is a well-known important direct semiconductor with a band gap of 3.66 eV[22,29] that can be used for in vivo bioapplications because of its low toxicity.[30−32] Additionally, ZnS is useful for nonlinear optical devices, sensor, lasers, and flat display fields because of its remarkable optical and electrical properties.[2,33] However, the major problem associated with ZnS is its high band gap, as well as its low QY. Different attempts have been made to improve the QY of ZnS nanoparticles, including the incorporation of low band gap materials or metals as dopant[22,28] and the formation of a surface layer with any low band gap band semiconductor or other materials in the form of core/shell particles.[23,24,30,34] In recent work, it was observed that the doping of Bi and Au[25,35] on hollow ZnS nanoparticles also enhances the optical and catalytic properties. To the best of our knowledge, ZnS-based hollow multishell (two or more shell layers) nanoparticles have not been studied, but ZnS-based

Received: August 13, 2013
Revised: September 29, 2013
Published: October 4, 2013

multilayer core/shell nanoparticles with CdS or CdSe have been well-studied by different research groups.[34,36−38] Ag_2S is another important semiconductor material which has a low (∼1.0 eV) band gap[39,40] and is frequently used in various electronics devices.[41] Because of the low toxicity of both materials, the combination of these can be utilized for biomedical applications. It has also been observed that hollow nanospheres have a broad range of potential applications in catalysis or in the biomedical field compared to those of solid spheres because of the higher specific surface area[42−44] and because it is easy to load the drug within the cavity for specific, controlled drug release.[45−50]

Reports from literature have shown that either metal or low band gap chalcogenide semiconductor materials have been incorporated as a dopant or inner/outer shell layer in the ZnS-based core/shell structure to enhance their optical properties. The main motivation of the present study is to increase the photoluminescence properties of ZnS particles by the addition of a suitable material in the form of a hollow nanostructure and to understand the mechanism of particle formation and the enhancement in optical properties. To achieve this, first we report an easy, novel method for the synthesis of hollow double-shell semiconductor nanoparticles. Second, the effect of the sequence of materials and their shell layer thickness on QY and photoluminescence (PL) properties was also studied and compared with that of single hollow particles. This study is novel because to the best of our knowledge a similar approach to enhance the QY and PL of ZnS has not yet been reported. The Ag_2S was chosen to improve the QY because of its higher QY than that of ZnS. In the literature, it has been shown that CdS and CdSe can also be used, but Cd compounds are much more toxic than Ag_2S for in vivo biological applications.[51]

EXPERIMENTAL SECTION

Materials. The required chemicals were purchased from the following sources: sodium thiosulphate ($Na_2S_2O_3$, $5H_2O$) from Rankem, cetyltrimethyl ammonium bromide (CTAB) with 99% purity from Sigma Aldrich, nitric acid (HNO_3) from Merck, $AgNO_3$ with 99.9% purity from Ranbaxy, [$Zn(NO_3)_2$ $6H_2O$] (96−103% assay) from Merck, and carbon disulfide (CS_2) with 99% purity from Merck. All the chemicals were used as received without any further purification. Ultrapure water with 18.2 MΩ cm resistivity, 71.5 mN/m surface tension, and a pH of 6.4−6.5 was used for all the experiments. The constant temperature of 28 ± 0.5 °C was maintained throughout the experiments.

Synthesis Techniques. Sulfur nanoparticles were synthesized as cores from a HNO_3-catalyzed reaction of sodium thiosulphate in the presence of a CTAB solution according to our previous study.[52] After the completion of core formation, the solution was sonicated by a probe-type sonicator using 260W for 20 min, and then finally, for the first shell coating, the precursors [either $AgNO_3$ or $Zn(NO_3)_2$ for Ag_2S and ZnS, respectively] were slowly added stepwise to the solution with constant stirring in the presence of S^{2-} ions. After a waiting period of 60 min for completion of the reaction, the solution was soincated by a probe sonicator using 150W for 15 min, and next, the precursors [alternatively either $AgNO_3$ or $Zn(NO_3)_2$ depending on the external shell material] were added for final external coating to the solution in situ without separating the particles. Then, the particles were separated by centrifugation at 25 000 rpm for 20 min, washed thrice by a water−ethanol mixture (1:1, v/v), and finally, the collected washed solid materials were dried overnight in a hot air oven at 55 °C and calcined at 450 °C for 30 min in air to remove the sulfur for the formation of multishell hollow particles.

Particle Characterization. Particle size measurement was carried out by dynamic light scattering (DLS) using a Malvern Zeta Size analyzer (Nano ZS) with the help of cumulant fitting model and intensity distribution within the media. The size and shape of the particles were observed under a scanning electron microscope (JEOL JSM-6480LV) and a transmission electron microscope (Tecnai S-twin). Hollow particles were also characterized by UV−Vis−NIR spectroscopy (Shimadzu-3600), fluorescence spectroscopy (Hitachi-7000), and X-ray diffraction (Philips, PW 1830 HT).

RESULT AND DISCUSSION

Characterization of Particles by UV−Vis Spectroscopy. Initially, after the formation of different hollow particles, their light absorption properties were preliminary characterized by UV−vis spectroscopy, which are characteristic of individual materials in a certain wavelength region. The absorption spectra of the hollow Ag_2S, ZnS/Ag_2S, Ag_2S/ZnS, and ZnS nanoparticles are shown in Figure 1. The figure shows that the

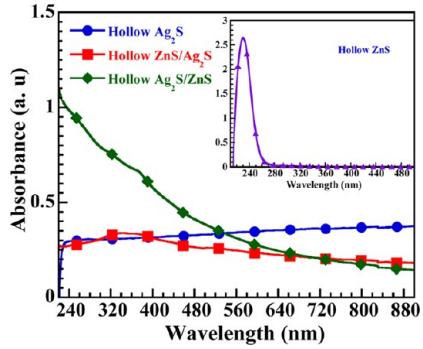

Figure 1. Absorbance spectra of hollow Ag_2S, ZnS/Ag_2S, Ag_2S/ZnS, and ZnS nanoparticles.

absorbance spectrum of the hollow Ag_2S particles has a higher absorbance intensity than that of other three spectra in the visible region because of its low band gap (∼1 eV), and hollow ZnS shows a high intensity absorbance peak in the UV range at the 231 nm wavelength (inset of Figure 1). However, when hollow Ag_2S particles are externally coated with ZnS, the pattern of the absorbance spectrum is different than that of hollow ZnS particles (as shown in the inset of Figure 1). The absorbance intensity of hollow Ag_2S/ZnS particles increases in the UV region without any specific peak with respect to that of hollow Ag_2S, but the intensity is lower than that of hollow ZnS nanoparticles and shows a shoulder at 360 nm because of the external shell coating of the high band gap ZnS material (∼3.66 eV) on the low band gap Ag_2S; therefore, ZnS is directly exposed to the imposed light that influences the absorption spectrum. The increase in absorbance in the visible region is mainly because of the influence of the internal Ag_2S shell, but the magnitude is lower than that of pure hollow Ag_2S particles because of the presence of the thick ZnS layer (∼28 nm). Generally, when the outer shell layer thickness is greater, the incident light cannot completely penetrate the layer. On the other hand, when the sequence of materials is reversed, in contrast to hollow Ag_2S/ZnS, the absorbance pattern of the hollow ZnS/Ag_2S nanoparticles is different; the absorbance intensity is high at the extended visible region (above the 710

dx.doi.org/10.1021/jp408105m | J. Phys. Chem. C 2013, 117, 23385−23390

nm wavelength) because of the presence of low band gap Ag_2S in the external shell. At the same time, because the external shell thickness of Ag_2S is ~23.3 nm, it is expected that ZnS has a partial effect on the absorbance intensity of hollow ZnS/Ag_2S particles; therefore, in the UV region, the absorbance is quite low compared to that of hollow ZnS or hollow Ag_2S/ZnS particles. Additionally, the spectrum does not match with the hollow Ag_2S nanoparticles in the visible range. Hollow ZnS/Ag_2S nanoparticles show a broad band with a wide peak at 330−360 nm, and the absorbance in the visible region is again lower compared to that of hollow Ag_2S nanoparticles. This behavior can be attributed to the formation of a ZnS and Ag_2S complex at the interface (which is confirmed from the XRD analysis). The complex formation at the interface leads to a change in the energy positions of the valence and conduction band of the double-layer hollow particles. As a result, while individual layer (external and internal) thicknesses are low, the complex structure at the interface influences the absorbance spectrum of both double-layer hollow particles and shows a different absorbance spectrum pattern than that of Ag_2S or ZnS nanoparticles in the 330−370 nm region.

Characterization of Particles by XRD. The XRD patterns of both double-shell hollow particles are shown in Figure 2. In

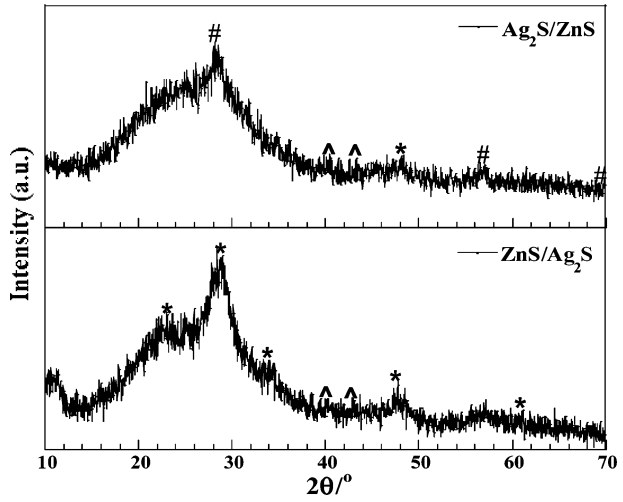

Figure 2. XRD patterns of hollow Ag_2S, ZnS, Ag_2S/ZnS, and ZnS/Ag_2S particles [hexagonal Ag_2S (*), hexagonal ZnS (#), and monoclinic zinc silver thiocyanate (^)].

our previous study,[41] it was observed that the hollow Ag_2S particles formed by this route are in monoclinic phase with interplanar spacing of 0.261 nm (Note: [220] plane lattice spacing for monoclinic Ag_2S is 0.260 nm). In the present study, for hollow Ag_2S/ZnS particles after the coating of ZnS over Ag_2S, peaks for Ag_2S disappear and new peaks are observed because of cubic ZnS (02-0564 from the JCPDS PDF number) with interplanar spacing of 0.311 nm (Note: [111] plane lattice spacing for cubic ZnS is 0.312 nm). Similarly, in the case of hollow ZnS/Ag_2S particles, when the internal ZnS shell is coated with Ag_2S, the XRD pattern shows only monoclinic Ag_2S (09-0422 from the JCPDS PDF number). Therefore, these results support the formation of a thick double-shell coating on the core surface. Interestingly, it is observed that there is a common XRD peak of monoclinic zinc silver thiocyanate [$Zn(Ag(SCN)_2)_2$] (76-2302 from the JCPDS PDF number) for both hollow particles, which is attributed to the formation of this complex during the removal of the core (S) by calcinations at 450 °C.

Characterization of Particles by FESEM and TEM. FESEM and TEM images of both double-shell hollow nanoparticles are shown in Figures 3 and 4. Similar to hollow

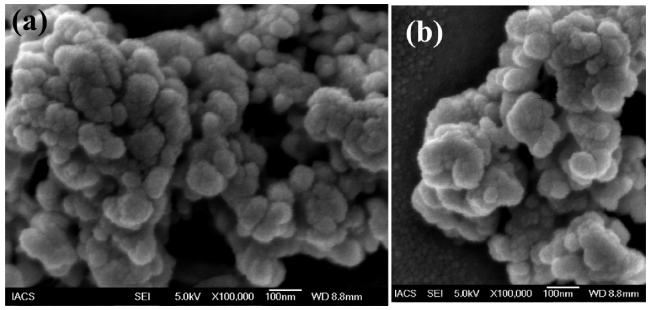

Figure 3. FESEM images of hollow (a) Ag_2S/ZnS and (b) ZnS/Ag_2S nanoparticles.

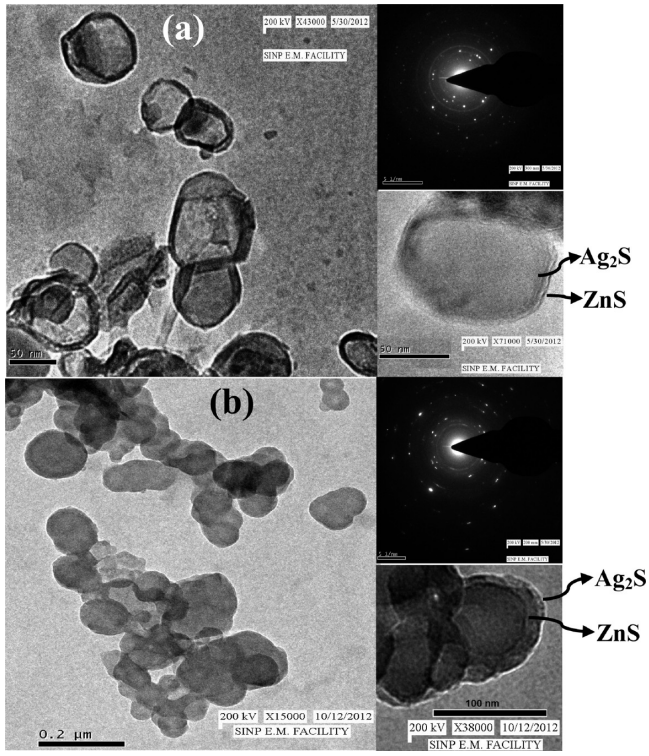

Figure 4. Electron diffraction patterns and higher resolution images of hollow (a) Ag_2S/ZnS and (b) ZnS/Ag_2S nanoparticles.

Ag_2S nanoparticles,[41] in the case of both double-shell hollow particles, the external shell layer is formed by the deposition of small-sized particles so that the outer surface of the particles is not exceptionally smooth, which is confirmed by the FESEM analysis, as shown in Figure 3a,b. The TEM images (as shown in Figure 4a,b) confirm the shape of the particles; both particles are nearly spherical in structure. The size range of these particles is ~80−85 nm, as obtained by DLS analysis, with a good agreement with TEM images (measured randomly for selected individual particles). In both cases (hollow Ag_2S/ZnS and ZnS/Ag_2S nanoparticles), the shell thickness of Ag_2S and ZnS is in the ~5−10 nm range after the removal of the core by calcination.

dx.doi.org/10.1021/jp408105m | J. Phys. Chem. C 2013, 117, 23385−23390

Characterization of Particles by Fluorescence Spectroscopy. Fluorescence spectroscopy is another characterization technique that gives useful information about the band gap and QY, which are very important properties for a semiconductor material. The light emission properties of the material are important factors for the application of these semiconductor materials in optical imaging or in sensors that is mainly associated with the type of semiconductor (direct or indirect) material and its band gap. Normally, the light emission time span of the material decreases with a lowering in the band gap, and, as a result, low band gap materials emit light for a short time (picoseconds or nanoseconds) while excited. Generally, these materials are not suitable for application in optical imaging, but when a low band gap material is coated with a single-layer high band gap material in the form of core/shell nanoparticles, electrons are located in the core, whereas holes are located throughout the core and shell layer so that the QY increases because of the passivation of the core surface and the elimination of the surface trap states. However, when the external layer thickness increases from a single layer of molecules to bi-, tri-, or even multiple layer, the QY decreases because of the crystal strain induced in the heterostructure with increasing shell thickness, which may cause new surface traps or crystallographic defects.[53] Fluorescence spectra of hollow Ag_2S, ZnS, and double-shell hollow Ag_2S/ZnS and ZnS/Ag_2S particles are shown in Figure 5. The QY of the hollow Ag_2S nanoparticles increases to a greater extent compared to that of solid Ag_2S synthesized by the same route as reported before.[41] In the present study, (see Table S1 SI) the QY of Ag_2S decreases from 89 to 39% when coated with ZnS (27.8 nm thickness), but the QY of this double-shell particle is higher than that of pure hollow ZnS particles (14%) synthesized by the same technique, which may have a better application scope in optical imaging and sensors because of the enhancement of QY. The result can be attributed to the fact that the coating of ZnS passivates the emission of Ag_2S. On the other hand, the presence of the internal layer of Ag_2S influences the emission of ZnS, which in turn increases the QY of hollow Ag_2S/ZnS nanoparticles higher than that of simple hollow ZnS nanoparticles. As observed in Table S2 (see SI), the QY depends on the thickness of the external shell layer. When the thickness of ZnS is low (16.4 nm), the QY is less (19%). With an increase in thickness (27.8 nm), the QY increases (39%), but with a further increase in thickness, the QY again decreases (30%). Notably, a similar trend was observed by Dabbousi et al.[54] for CdSe/ZnS core/shell nanoparticles. When Ag_2S is coated with high band gap ZnS, the emission of Ag_2S passivates because of the presence of both an intermixing layer as well as a thick external ZnS layer, which in turn reduces the QY. Initially, when the ZnS shell thickness is low, there is a possibility of mixing between both layers at the interface, and as a result, radiative transition decreases and QY also decreases. In this case, when the external shell thickness is sufficiently large, in spite of mixing between two layers at the interface, the external shell layer is sufficiently thick to passivate the emission of the core Ag_2S. As a result, QY and stability increase, which in turn is reflected in the fluorescence decay profile of hollow Ag_2S/ZnS and ZnS/Ag_2S nanoparticles (as shown in Figure S1, SI), because in the case of hollow Ag_2S/ZnS nanoparticles, the emission decay is still observed in a millisecond time frame. However, in the case of hollow ZnS/Ag_2S nanoparticles, in a millisecond time domain, only residual intensity was observed. So it is expected that the emission is slower for hollow Ag_2S/ZnS nanoparticles than that of hollow ZnS/Ag_2S nanoparticles because of the presence of the external ZnS layer. The decreasing QY because of the thick shell layer of higher band gap materials was also observed for CdSe/ZnS and CdTe/CdS core/shell nanoparticles.[53,54] In the case of double-shell hollow ZnS/Ag_2S nanoparticles, the coating of low band gap material (Ag_2S) on the high band gap materials (ZnS) results in a 21% increase in QY compared to the pure ZnS particles (14%), but the value is still lower compared to the pure hollow Ag_2S nanoparticles. It is noteworthy to mention that an extra peak is observed at a wavelength of 300.4 nm (corresponding to 4.13 eV) for hollow ZnS, Ag_2S/ZnS, and ZnS/Ag_2S nanoparticles because of the quantum confinement effect of small-sized ZnS particles deposited during the formation of the shell layer. This peak appears at a higher wavelength than the corresponding band gap of bulk ZnS materials (3.66 eV). The intensity of the peak follows a decreasing sequence of hollow ZnS > hollow Ag_2S/ZnS > hollow ZnS/Ag_2S particles. There was no extra peak observed for hollow Ag_2S particles.

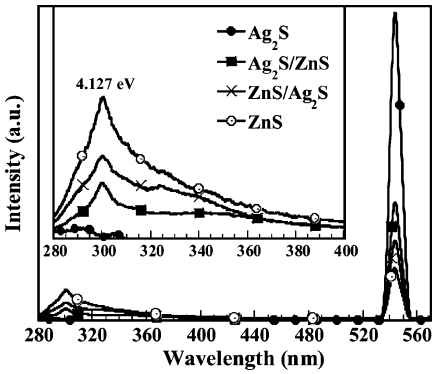

Figure 5. Emission spectra of hollow Ag_2S, Ag_2S/ZnS, ZnS/Ag_2S, and ZnS nanoparticles.

During the synthesis of multishell semiconductor materials, epitaxial growth is one mechanism reported by many researchers.[24,53,54] In general, epitaxial growth is preferable for minimizing the surface defects and electron mobility which increase the optical properties of these materials. However, in general, this epitaxial growth is possible when there is a lattice mismatch within 5%. In this case, Ag_2S and ZnS both are in different structures, and the lattice planes are also different [(ZnS: Cubic, lattice spacing 0.311 nm) and (Ag_2S: monoclinic, lattice spacing 0.261 nm)] with a large difference in lattice spacing; therefore, it is expected that the second shell will grow on the first shell though nonepitaxial growth. As there is no discrete interface between the two shell layers, electron mobility through the interface possibly decreases, and as a result, the optical properties decrease drastically when Ag_2S is coated with ZnS. These hollow Ag_2S/ZnS or ZnS/Ag_2S particles are optically more active than pure hollow ZnS particles due the presence of the more optically active Ag_2S, and generally, these materials are more useful for biomedical application in vivo and for use as chemical detectors[27,28] because both Ag_2S and ZnS are less toxic.[23,30]

CONCLUSIONS

In conclusion, we report a simple sulfur-template-based sacrificial core removal technique for the synthesis of double-shell hollow ZnS/Ag_2S and Ag_2S/ZnS nanoparticles to improve the QY of ZnS. ZnS is an important material for optical imaging

dx.doi.org/10.1021/jp408105m | J. Phys. Chem. C 2013, 117, 23385−23390

and sensor applications, but the limitation of simple hollow ZnS particles is its low QY (0.14). The presence of Ag_2S in the form of a double-shell hollow particle enhances the QY, enhances the light emission properties, and improves the possibility of novel application. The presence of Ag_2S as an inner shell is more effective than as an outer shell to enhance the QY; the enhancements are 25 and 7% more, respectively, for the inner and outer Ag_2S shell compared to the pure hollow ZnS particles. The QY of hollow Ag_2S/ZnS nanoparticles also depends on the thickness of the ZnS layer, and it is maximum at a certain shell thickness, but below and above that thickness, the QY decreases because of either the intermixing of two layers or the passivation of emission of the Ag_2S layer because of the thicker ZnS shell layer.

■ ASSOCIATED CONTENT

Ⓢ Supporting Information

Quantum yield calculation method, Table S1, Table S2, and fluorescence decay profile. This information is available free of charge via the Internet at http://pubs.acs.org.

■ AUTHOR INFORMATION

Corresponding Author

*E-mail: santanuparia@yahoo.com. Fax: +91 661 246 2999.

Notes

The authors declare no competing financial interest.

■ ACKNOWLEDGMENTS

The financial support from the Department of Science and Technology (DST) under Nanomission, New Delhi, India, Grant No. SR/S5/NM-04/2007 and CSIR, New Delhi, India, Grant No. 22(0527)/10/EMR-II, for this project are gratefully acknowledged. We also acknowledge the Saha Institute of Nuclear Physics (SINP) and the Indian Association for the Cultivation of Science (IACS), Kolkata, India, for giving us the opportunity to access their TEM and FESEM facility, respectively.

■ REFERENCES

(1) Zhang, H.; Zhang, X.; Yang, X. Facile Synthesis of Monodisperse Polymer/SiO_2/Polymer/TiO_2 Tetra-layer Microspheres and the Corresponding Double-Walled Hollow SiO_2/TiO_2 Microspheres. *J. Colloid Interface Sci.* **2010**, *348*, 431−440.

(2) Yu, J.; Zhang, J.; Liu, S. Ion-Exchange Synthesis and Enhanced Visible-light Photoactivity of CuS/ZnS Nanocomposite Hollow Spheres. *J. Phys. Chem. C* **2010**, *114*, 13642−13649.

(3) Agrawal, M.; Gupta, S.; Pich, A.; Zafeiropoulos, N. E.; Stamm, M. A Facile Approach to Fabrication of ZnO−TiO_2 Hollow Spheres. *Chem. Mater.* **2009**, *21*, 53543−53548.

(4) Chen, B.; Deng, J.; Yang, W. Hollow Two-Layered Chiral Nanoparticles Consisting of Optically Active Helical Polymer/Silica: Preparation and Application for Enantioselective Crystallization. *Adv. Funct. Mater.* **2011**, *21*, 2345−2350.

(5) Xia, X.-M.; Yu, P.; Peng, N.; Zhang, Y.; Xue, Y.-N.; Zhuo, R.-X.; Huang, S.-W. Tunable Release of Biomacromolecules from Reductive-Responsive Multilayered Hollow Microcapsules. *J. Controlled Release* **2011**, *152*, e101−e103.

(6) Zhao, X.; Du, P.; Liu, P. Preparation of Aggregation-Resistant Biocompatible Superparamagnetic Noncovalent Hybrid Multilayer Hollow Microspheres for Controlled Drug Release. *Mol. Pharmaceutics* **2012**, *9*, 3330−3339.

(7) Wu, Y.; Wu, Z.; Lin, X.; He, Q.; Li, J. Autonomous Movement of Controllable Assembled Janus Capsule Motors. *ACS Nano* **2012**, *6*, 10910−10916.

(8) Sun, J.; Zhang, J.; Zhang, M.; Antonietti, M.; Fu, X.; Wang, X. Bioinspired Hollow Semiconductor Nanospheres as Photosynthetic Nanoparticles. *Nat. Commun* **2012**, 1139.

(9) Ghosh Chaudhuri, R.; Paria, S. Core/Shell Nanoparticles: Classes, Properties, Synthesis Mechanisms, Characterization, and Applications. *Chem. Rev.* **2012**, *112*, 2373−2433.

(10) Reiss, P.; Protiere, M.; Li, L. Core/Shell Semiconductor Nanocystals. *Small* **2009**, *5*, 154−168.

(11) Trikalitis, P. N.; Rangan, K. K.; Bakas, T.; Kanatzidis, M. G. Varied Pore Organization in Mesostructured Semiconductors Based on the $[SnSe_4]^{4+}$ Anion. *Nature* **2001**, *410*, 671−675.

(12) Dorfs, D.; Henschel, H.; Kolny, J.; Eychmüller, A. Multilayered Nanostrucutres: Theory and Experiment. *J. Phys. Chem. B* **2004**, *108*, 1578−1583.

(13) Blackman, B.; Battaglia, D.; Peng, X. Bright and Water-Soluble Near IR-Emitting CdSe/CdTe/ZnSe Type-II/Type-I Nanocrystals, Tuning the Efficiency and Stability by Growth. *Chem. Mater.* **2008**, *20*, 4847−4853.

(14) Eychmüller, A.; Mews, A.; Weller, H. A Quantum Dot Quantum Well: CdS/HgS/CdS. *Chem. Phys. Lett.* **1993**, *208*, 59−62.

(15) Kim, D. W.; Cho, K.; Kim, H.; Park, B.; Sung, M. Y.; Kim, S. Optoelectronic Characteristics of CdSe/HgTe/CdTe Quantum-Dot Quantum-Well Nanoparticles. *Solid. State Commun.* **2006**, *140*, 215−218.

(16) Kim, S. W.; Zimmer, J. P.; Ohnishi, S.; Tracy, J. B.; Frangioni, J. V.; Bawendi, M. G. Engineering $InAs_xP_{1-x}$/InP/ZnSe III-V Alloyed Core/shell Quantum Dots for the Near-Infrared. *J. Am. Chem. Soc.* **2005**, *127*, 10526−10532.

(17) Lifshitz, E.; Porteanu, H.; Glozman, A.; Weller, H.; Pflughoefft, M.; Echymüller, A. Optically Detected Magnetic Resonance Study of CdS/HgS/CdS Quantum Dot Quantum Wells. *J. Phys. Chem. B* **1999**, *103*, 6870−6875.

(18) Wang, D.-W.; Zhu, X.-M.; Lee, S.-F.; Chan, H.-M.; Li, H.-W.; Kong, S. K.; Yu, J. C.; Cheng, C. H. K.; Wang, Y.-X. J.; Leung, K. C.-F. Folate-Conjugated Fe_3O_4@SiO_2@gold Nanorods@mesoporous SiO_2 Hybrid Nanomaterial: A Theranostic Agent for Magnetic Resonance Imaging and Photothermal Therapy. *J. Mater. Chem. B* **2013**, *1*, 2934−2942.

(19) Wang, Y.; Sun, H.; Zhang, T.; Shen, Y.; Zhang, J.; Xia, J.; Xie, A. Synthesis and Property of Multifunctional Fe_3O_4@SiO_2@CeO_2@Au Composite Microspheres. *Nano* **2012**, *7*, 1250042.

(20) Zhu, M. Q.; Han, J. J.; Li, A. D. Q. CdSe/CdS/SiO_2 Core/Shell/Shell Nanoparticles. *J. Nanosci. Nanotechnol.* **2007**, *7*, 2343−2348.

(21) Dai, Z.; Möhwald, H.; Tiersch, B.; Dähne, L. Nanoengineering of Polymeric Capsules with a Shell-in-Shell Structure. *Langmuir* **2002**, *18*, 9533−9538.

(22) Iqbal, M. J.; Iqbal, S. Synthesis of Stable and Highly Luminescent Beryllium and Magnesium Doped ZnS Quantum Dots Suitable for Design of Photonic and Sensor Material. *J. Lumin.* **2013**, *134*, 739−746.

(23) Patolsky, F.; Gill, R.; Weizmann, Y.; Mokari, T.; Banin, U.; Willner, I. Lighting-up the Dynamics of Telomerization and DNA Replication by CdSe-ZnS Quantum Dots. *J. Am. Chem. Soc.* **2003**, *125*, 13918−13919.

(24) Snee, P. T.; Somers, R. C.; Nair, G.; Zimmer, J. P.; Bawendi, M. G.; Nocera, D. G. A Ratiometric CdSe/ZnS Nanocrystal pH Sensor. *J. Am. Chem. Soc.* **2006**, *128*, 13320−13321.

(25) Shuai, Y.; Liu, C.; Wang, J.; Cui, X.; Nie, L. Pseudo-Bi-Enzyme Glucose Sensor: ZnS Hollow Spheres and Glucose Oxidase Concerted Catalysis Glucose. *Analyst* **2013**, *138*, 3259−3263.

(26) Li, Z.; Ma, J.; Zong, Y.; Men, Y. ZnS Nanoparticles for High-Sensitive Fluorescent Detection of Pyridine Compounds. *J. Alloys Comp.* **2013**, *559*, 39−44.

(27) Goldman, E. R.; Medintz, I. L.; Whitley, J. L.; Hayhurst, A.; Clapp, A. R.; Uyeda, H. T.; Deschamps, J. R.; Lassman, M. E.; Mattaoussi, H. A Hybrid Quantum Dot-Antibody Fragment Fluorescence Resonance Energy Transfer-Based TNT Sensor. *J. Am. Chem. Soc.* **2005**, *127*, 6744−6751.

(28) Dong, B.; Cao, L.; Su, G.; Liu, W.; Qu, H.; Jiang, D. Synthesis and Characterization of the Water-Soluble Silica-Coated ZnS:Mn Nanoparticles as Fluorescent Sensor for Cu^{2+} Ions. *J. Colloid Interface Sci.* **2009**, *339*, 78−82.
(29) Qu, H.; Cao, L.; Su, G.; Liu, W. Effect of Inorganic Shells on Luminescence Properties of ZnS:Ag Nanoparticles. *J. Mater. Sci.* **2013**, *48*, 4952−4961.
(30) Liu, Y.-S.; Sun, Y.; Vernier, P. T.; Liang, C.-H.; Chong, S. Y. C.; Gundersen, M. A. pH-Sensitive Photoluminescence of CdSe/ZnSe/ZnS Quantum Dots in Human Ovarian Cancer Cells. *J. Phys. Chem. C* **2007**, *111*, 2872−2878.
(31) Hu, J.-S.; Ren, L.-L.; Guo, Y.-G.; Liang, H.-P.; Cao, A.-M.; Wan, L.-J.; Bai, C.-L. Mass Production and High Photocatalytic Activity of ZnS Nanoporous Nanoparticles. *Angew. Chem., Int. Ed.* **2005**, *44*, 1269−1273.
(32) Zhang, Y.; Liu, W.; Wang, R. From ZnS Nanoparticles, Nanobelts, to Nanotetrapods: The Ethylenediamine Modulated Anisotropic Growth of ZnS Nanostructures. *Nanoscale* **2012**, *4*, 2394−2399.
(33) Moore, D.; Wang, Z. L. Growth of Anisotropic One-Dimensional ZnS Nanostructures. *J. Mater. Chem.* **2006**, *16*, 3898−3905.
(34) Talapin, D. V.; Mekis, I.; Gotzinger, S.; Kornowski, A.; Benson, O.; Weller, H. CdSe/CdS/ZnS and CdSe/ZnSe/ZnS Core−Shell−Shell Nanocrystals. *J. Phys. Chem. B* **2004**, *108*, 18826−18831.
(35) Zhang, J.; Liu, S.; Yu, J.; Jaroniec, M. A Simple Cation Exchange Approach to Bi-Doped ZnS Hollow Spheres with Enhanced UV and Visible-Light Photocatalytic H_2-Production Activity. *J. Mater. Chem.* **2011**, *21*, 14655−14662.
(36) Little, R. B.; EI-Sayed, M. A.; Bryant, G. W.; Burke, S. Formation of Quantum Dot Quantum Well Heteronanostructures with Large Lattice Mismatch: ZnS/CdS/ZnS. *J. Chem. Phys.* **2001**, *114*, 1813−1822.
(37) Park, J. J.; Lacerda, S. H. D. P.; Stanley, S. K.; Vogel, B. M.; Kim, S.; Douglas, J. F.; Rahgavan, D.; Karim, A. Langmuir Adsorption Study of the Interaction of CdSe/ZnS Quantum Dots with Madel Substrates: Influence of Substrate Surface Chaemistry and pH. *Langmuir* **2009**, *25*, 443−450.
(38) Xie, R.; Kolb, U.; Li, J.; Basche, T.; Mews, A. Synthesis and Characterization of Highly Luminescent CdSe-Core CdS/Zn0.5Cd0.5S/ZnS Multishell Nanocrystals. *J. Am. Chem. Soc.* **2005**, *127*, 7480−7488.
(39) Meziani, M. J.; Sun, Y. P. Protein-Conjugated Nanoparticles from Rapid Expansion of Supercritical Fluid Solution into Aqueous Solution. *J. Am. Chem. Soc.* **2003**, *125*, 8015−8018.
(40) Liu, J.; Raveendran, P.; Shervani, Z.; Ikushima, Y. Synthesis of Ag_2S Quantum in Water-in-CO2 Microemulsions. *Chem. Commun.* **2004**, 2582−2583.
(41) Ghosh Chaudhuri, R.; Paria, S. A Novel Method for the Templated Synthesis of Ag_2S Hollow Nanospheres in Aqueous Surfactant Media. *J. Colloid Interface Sci.* **2012**, *369*, 117−122.
(42) Chen, H. M.; Liu, R. S.; Lo, M. Y.; Chang, S. C.; Tsai, L. D.; Peng, Y. M.; Lee, J. F. Hollow Platinum Spheres with Nano-Channels: Synthesis and Enhanced Catalysis for Oxygen Reduction. *J. Phys. Chem. C* **2008**, *112*, 7522−7526.
(43) Caruso, F. Hollow Capsule Possessing through Colloidal Templating and Self Assembly. *Chem.—Eur. J.* **2000**, *6*, 413−419.
(44) Caruso, F.; Caruso, R. A.; Mohwald, H. Nanoengineering of Inorganic and Hybrid Hollow Spheres by Colloidal Templating. *Science* **1998**, *282*, 1111−1114.
(45) Son, S. J.; Bai, X.; Lee, S. B. Inorganic Hollow Nanoparticles and Nanotubes in Nanomedicine Part 1. Drug/Gene Delivery Applications. *Drug Discovery Today* **2007**, *12*, 650−656.
(46) Huang, H.; Remsen, E. E.; Kowalewski, T.; Wooley, K. L. Nanocages Derived from Shell Cross-Linked Micelle Templates. *J. Am. Chem. Soc.* **1999**, *121*, 3805−3806.
(47) Dinsmore, A. D.; Hsu, M. F.; Nikolaides, M. G.; Marquez, M.; Bausch, A. R.; Weitz, D. A. Colloidosomes: Selectively Permeable Capsules Composed of Colloidal Particles. *Science* **2002**, *298*, 1006−1009.
(48) Luo, S.-C.; Jiang, J.; Liour, S. S.; Gao, S.; Ying, J. Y.; Yu, H.-H. Magnetic PEDOT Hollow Capsules with Single Holes. *Chem. Commun.* **2009**, 2664−2666.
(49) Gao, Y.; Chen, Y.; Ji, X.; He, X.; Yin, Q.; Zhang, Z.; Shi, J.; Li, Y. Controlled Intracellular Release of Doxorubicin in Multidrug-Resistant Cancer Cells by Tuning the Shell-Pore Sizes of Mesoporous Silica Nanoparticles. *ACS Nano* **2011**, *5*, 9788−9798.
(50) He, Q.; Wu, Z.; Huang, C. Hollow Magnetic Nanoparticles: Synthesis and Applications in Biomedicine. *J. Nanosci. Nanotechnol.* **2012**, *12*, 2943−2954.
(51) Zhang, Y.; Hong, G.; Zhang, Y.; Chen, G.; Li, F.; Dai, H.; Wang, Q. Ag_2S Quantum Dot: A Bright and Biocompatible Fluorescent Nanoprobe in the Second Near-Infrared Window. *ACS Nano* **2012**, *6*, 3695−3702.
(52) Ghosh Chaudhuri, R.; Paria, S. Synthesis of Sulfur Nanoparticles in Aqueous Surfactant Solutions. *J. Colloid Interface Sci.* **2010**, *343*, 439−446.
(53) Dorfs, D.; Franzl, T.; Osovsky, R.; Brumer, M.; Lifshitz, E.; Klar, T. A.; Eychmuller, A. Type-I and Type- II Nanoscale Heterostructures Based on CdSe Nanocrystals: A Comparative Study. *Small* **2008**, *4*, 1148−1152.
(54) Dabbousi, B. O.; Rodriguez-Viejo, J.; Mikulec, F. V.; Heine, J. R.; Mattoussi, H.; Ober, R.; Jensen, K. F.; Bawendi, M. G. (CdSe)ZnS Core-Shell Quantum Dots: Synthesis and Characterization of a Series of Highly Luminescent Nanocrystallites. *J. Phys. Chem. B* **1997**, *101*, 9463−9475.